ORIGINAL ARTICLE

Noninvasive Diagnosis of Oral Neoplasia Based on Fluorescence Spectroscopy and Native Tissue Autofluorescence

Ann Gillenwater, MD; Rhonda Jacob, DDS, MS; Ravi Ganeshappa, MD; Bonnie Kemp, MD; Adel K. El-Naggar, MD, PhD; J. Lynn Palmer, PhD; Gary Clayman, MD, DDS; Michele Follen Mitchell, MD; Rebecca Richards-Kortum, PhD

Objective: To evaluate the clinical potential of fluorescence spectroscopy (a noninvasive technique for assessing the chemical and morphologic composition of tissue) for in vivo detection of oral cavity neoplasia.

Design: A fluorescence spectroscopy system recorded spectra from oral cavity sites in 8 healthy volunteers and in 15 patients with premalignant or malignant oral cavity lesions at 337-, 365-, and 410-nm excitation wavelengths in the emission range of 350 to 700 nm. Fluorescence peak intensities and spectral line shapes were compared and diagnostic algorithms were developed to distinguish normal sites from abnormal sites.

Setting: The head and neck cancer clinic at a tertiary referral center in Houston, Tex.

Results: Differences were found in spectra from normal, dysplastic, and malignant oral mucosa. The fluorescence intensity of normal mucosa was greater than that of abnormal areas. In addition, the ratio of red region (635-nm) to blue region (455-490-nm) intensities was greater in abnormal areas. Diagnostic discrimination was achieved when test site spectra were compared with spectra from a normal site in the same patient. One diagnostic algorithm based on spectra at 337 nm gave a sensitivity of 88% and a specificity of 100%.

Conclusions: Consistent differences exist between the fluorescence spectra of abnormal and normal oral mucosa. Therefore, fluorescence spectroscopy has the potential to improve the noninvasive diagnosis of oral cavity neoplasia. Further studies will better define the role of this technique in the detection of premalignant and early oral cancer lesions.

Arch Otolaryngol Head Neck Surg. 1998;124:1251-1258

From the Departments of Head and Neck Surgery (Drs Gillenwater, Jacob, and Clayman), Pathology (Drs Kemp and El-Naggar), Biomathematics (Dr Palmer), and Gynecologic Oncology (Dr Follen Mitchell), The University of Texas M. D. Anderson Cancer Center, Houston; and the Biomedical Engineering Program, The University of Texas, Austin (Drs Ganeshappa and Richards-Kortum).

PATIENTS WITH cancer of the oral cavity usually present when their disease is already advanced. Treatment for these patients vs those with early-stage disease is more disfiguring and debilitating, more expensive, and less successful. Early detection of neoplastic changes in the oral cavity has great potential for improving the quality of life and survival rates for patients. The goal of this study was to evaluate the clinical applicability of fluorescence spectroscopy (a noninvasive technique for assessing the chemical and morphologic composition of tissue) for the in vivo detection of oral cavity neoplasia.

Because of the accessibility of the oral cavity to examination and the fairly well-defined risk factors for malignancy, this area should be an ideal location to target for early cancer detection and prevention. The detection of oral cancer, however, relies heavily on clinical experience in recognizing suspicious lesions during physical examination. Detecting premalignant and early malignant lesions, and distinguishing them from more common benign inflammatory conditions, can be extremely difficult, even for experienced practitioners.

Several studies[1-3] have assessed the ability of vital staining with agents such as toluidine blue and Lugol iodine solution to improve diagnostic accuracy of clinical examinations. Although the sensitivity of application of these dyes was 90% or greater in many of these trials, specificity was lower. Most of these studies were conducted by clinicians who were experts in the diagnosis of malignant lesions in the oral cavity, and their results may not reflect the diagnostic predictability of these agents when used by less experienced personnel.

Current clinical practice requires an invasive biopsy with histological examination of abnormally appearing tissue to determine malignant potential. Practitioners and patients, however, are often reluctant to proceed with invasive biopsies of small, asymptomatic oral lesions. The development of a noninvasive and accurate method for real-time screening and diagnosis of oral

PARTICIPANTS AND METHODS

STUDY PARTICIPANTS

Eight healthy volunteers and 15 patients with a known or suspected premalignant or malignant oral cavity lesion were recruited at the Department of Head and Neck Surgery at The University of Texas M. D. Anderson Cancer Center, Houston. The study was reviewed and approved by the Internal Review Board of The University of Texas at Austin and by the Surveillance Committee at M. D. Anderson Cancer Center. Informed consent was obtained from each person in the study.

INSTRUMENTS

The spectroscopic system, as previously described,[5,6] incorporates a fiberoptic probe, 2 nitrogen-pumped dye lasers, and an optical multichannel analyzer. The probe consists of a central fiber surrounded by 6 fibers. Three fibers deliver excitation light at wavelengths of 337, 365, and 410 nm. Results of our in vitro analysis of head and neck squamous cell carcinoma specimens suggested that these wavelengths would produce the greatest discrimination between normal and abnormal tissue. The other 4 fibers collect the fluorescence emitted from the tissue. The probe illuminates a 1-mm-diameter spot on the tissue surface, and a quartz shield at the tip of the probe maintains a fixed distance between the fibers and the tissue. The laser has a 5-nanosecond pulse duration and a repetition rate of 30 Hz. The average transmitted pulse energies at 337, 365, and 410 nm were 15.2, 3.3, and 17.4 μJ, respectively.

The light from the 4 emission-collection fibers is sent to a polychromator, which disperses the light onto an array of diodes. The diodes collect and digitize the fluorescence to produce an emission spectrum.

CALIBRATION

A background spectrum, to be subtracted from the acquired patient data at the corresponding excitation wavelengths, was obtained at all 3 excitation wavelengths consecutively with the probe immersed in a nonfluorescent bottle filled with distilled water. Then, 1 fluorescence spectrum was measured at each excitation wavelength with the probe placed on the surface of a quartz cuvette containing a solution of rhodamine 610 dissolved in ethylene glycol (2 mg/L).

The detection system produces a nonuniform spectral response because the collection efficiency of the system is wavelength dependent. To correct for this, the spectrum of a known standard was recorded, and correction factors were derived from this spectrum. These factors were obtained by recording the spectrum of a National Institute of Standards and Technology traceable calibrated tungsten ribbon filament lamp. Corrected spectra from each site at each excitation wavelength were averaged and divided by the peak fluorescence intensity of the rhodamine 610 calibration standard at the corresponding excitation wavelength. Thus, the data illustrated in this article are not the absolute fluorescence intensities of the tissues but rather the intensities relative to the rhodamine 610 standard.

DATA ACQUISITION

The probe was disinfected with Metricide (Metrex Research Corp, Parker, Colo) before use in accordance with

lesions would have great potential for improving early detection of neoplastic changes, thereby improving the quality of life and survival rates for persons developing squamous cell carcinoma of the oral cavity.

Fluorescence spectroscopy is a new diagnostic modality with the potential to bridge this gap between clinical examination and invasive biopsy. Tissue architecture and biochemical composition can be evaluated in near real time using optical spectroscopy. By scanning the tissue with a small, flexible, fiberoptic probe, subtle alterations induced by dysplasia or inflammation can be detected noninvasively.[4] This is accomplished by analyzing the spectrum of the fluorescence emitted by the tissue. The development of software algorithms should allow automated data analysis of various types of spectra to provide instantaneous tissue diagnosis.

Studies of fluorescence spectroscopy for the diagnosis of neoplastic changes have been conducted in a variety of sites, including the gastrointestinal tract,[4] cervix,[5,6] lung,[7] and breast tissue.[8] Relatively fewer studies have been conducted on the oral mucosa.[9-11] Previously, we evaluated fluorescence spectra in vitro from specimens of head and neck squamous cell carcinoma over a broad spectrum of wavelengths. We found that the excitation wavelengths of 337, 365, and 410 nm produced the greatest separation between normal and abnormal spectra (data not shown). Results of a similar in vitro investigation by Dhingra et al[10] showed the greatest differences between normal and abnormal tissue samples at the 410-nm excitation wavelength. In the present study, we characterized fluorescence emission spectra obtained at 3 excitation wavelengths (337, 365, and 410 nm) from clinically normal, dysplastic, and cancerous oral mucosa and assessed the ability to discriminate between normal and abnormal sites by spectral alteration.

RESULTS

HEALTHY VOLUNTEERS

Fluorescence spectra were acquired from 95 sites in 8 healthy, nonsmoking volunteers.

Contralateral Sites—Same Subject

The peak fluorescence intensity at 337-nm excitation of contralateral sites on the lateral tongue in healthy volunteers is shown in **Figure 1**, A. Data from 2 volunteers are not shown in these figures because their spectra were only obtained unilaterally. In Figure 1, B, the peak intensity at each site has been normalized by the peak intensity of the right side in each patient (the left-side intensity was divided by the right-side intensity, making all right-sided intensities equal to 1). The average nor-

standard protocol. The probe was then guided into the oral cavity, and its tip was positioned flush with the mucosa. The probe projected the laser light onto the tissue surface at the 337-, 365-, and 410-nm excitation wavelengths sequentially. The tissue fluorescence was delivered through the collection fibers to the detection system where emission spectra were collected.

Five spectra for 5 consecutive pulses were measured at each excitation wavelength. Fluorescence spectra were obtained from each site at a resolution of 10 nm (full width at maximum) and a signal-to-noise ratio of approximately 30:1 at the fluorescence maximum at each excitation wavelength.

Fluorescence spectra were obtained from 8 healthy volunteers at 9 sites within the oral cavity (**Table 1**). In 6 of 8 volunteers, spectra were obtained bilaterally. No biopsy samples were obtained from volunteers.

In the 15 patients, a clinical diagnosis of each lesion as normal, abnormal (not dysplastic or dysplastic), or cancerous was recorded by an experienced head and neck surgeon (A.G.) or a dental oncologist (R.J.). Spectra were measured from clinically normal and abnormal oral sites in the clinic or in the operating room before surgical resection of oral lesions (**Table 2**). Spectra were obtained from sites within a lesion and from a contralateral, clinically normal site. After spectroscopy, a 2- to 4-mm biopsy specimen of the tissue was taken from where the probe measured the spectra. These specimens were evaluated by an experienced pathologist (B.K.) using light microscopy and were classified as normal, mucosal reactive atypia, dysplasia, or cancerous using a standard diagnostic criterion. Biopsy samples with multiple diagnoses were classified according to the most severe pathologic diagnosis. The pathologists and clinicians were unaware of the results of the spectroscopic analyses.

DATA ANALYSIS

Spectral data from the healthy volunteers were analyzed to determine the amount of variance in the fluorescence intensities and line shape of normal tissue (1) within a particular location in each subject, (2) among different anatomical locations in each subject, and (3) among subjects by site. Specifically, an analysis of the peak fluorescence intensities at the various sites and of the ratios of the intensities at the red (635-nm) and blue (455-490–nm) regions of the spectrum was made. An analysis of variance was performed to determine whether the average peak fluorescence intensity for all healthy volunteers differed among sites at each excitation wavelength.

Spectral data from patients were analyzed to detect variance in the fluorescence intensities and spectral line shape. For each patient, peak fluorescence intensities from abnormal sites were compared with those from normal sites. A similar comparison was made using a ratio of the fluorescence intensities at the red and blue regions. The intensity in the red region was measured at 635-nm emission for all excitation wavelengths because most red peaks occur at this wavelength. The intensity in the blue region was measured at 455 nm for 337- and 365-nm excitation wavelengths because most spectra produced a blue peak at 455 nm. At the 410-nm excitation wavelength, however, most of the peaks occurred at 490 nm; thus, the blue region data were measured at 490 nm for this excitation wavelength.

Abnormal samples were those histologically classified as mucosal reactive atypia, dysplasia, or cancer. Normal samples were those histologically classified as normal.

malized peak intensity of the left side was 1.06, with an SD of 0.21. We, therefore, chose 1.21 (1 plus 1 SD) as the cutoff value for normal with the peak fluorescence intensity at the 337-nm wavelength. Using the cutoff value, 4 of 6 normal sites were classified as normal.

The ratio of intensities at the red and blue spectral regions for spectra at each excitation wavelength were also compared; Figure 1, C and D, illustrate results at the 410-nm excitation. Figure 1, C, illustrates the red-blue intensity ratio of contralateral sites on the soft palate at the 410-nm excitation. In Figure 1, D, the red-blue intensity ratio has been normalized (the red-blue intensity ratio on the left side was divided by the right-side red-blue intensity ratio, making all right-sided ratios equal to 1). The average normalized red-blue intensity ratio of the left side was 1.12, with an SD of 0.33. We, therefore, chose 1.33 (1 plus 1 SD) as the cutoff value for normal using the red-blue intensity ratio at the 410-nm wavelength. Using this cutoff value, 4 of 5 normal sites were classified as normal. The red-blue intensity ratios in general showed less variation between sites or between patients than did the peak intensities; the least variation was observed at the 410-nm excitation wavelength.

Table 1. Comparison of Peak Intensities Among Different Oral Cavity Sites*

	Wavelength, nm		
Site	410	365	337
HP	0.71	0.77	1.70
SP	0.60	1.05	2.01
VT	0.55	0.58	1.71
RMT	0.51	0.86	1.79
FOM	0.47	0.76	1.65
BM	0.47	0.76	1.47
DT	0.26	0.36	1.07
LT	0.24	0.70	1.17
G	0.23	0.51	1.60

**The mean peak intensity for each site at each wavelength is shown. Wavelength 410: the 3 sites with highest mean peak intensities (HP, SP, and VT) were significantly greater than the 3 lowest (DT, LT, and G) at the .05 level of significance (or less). Also, the RMT mean was significantly greater than that of G. Wavelength 365: only the highest mean (SP) was significantly greater than the lower mean (DT). Wavelength 337: the mean peak intensity for SP was significantly greater than LT and DT, and the mean for RMT was significantly greater than DT. No other significant differences between mean peak intensities by sites were found. HP indicates hard palate; SP, soft palate; VT, ventral tongue; RMT, retromolar trigone; FOM, floor of mouth; BM, buccal mucosa; DT, dorsal tongue; LT, lateral tongue; and G, gingiva.*

Multiple Oral Sites

An analysis of variance was made separately for each wavelength (337, 365, and 410 nm) to determine whether the average peak fluorescence intensity differed among sites at each excitation wavelength. The independent variable of sites was significant for 2 of 3

Table 2. Patient Information Summary*

Patient No.	Site	Pathologic Diagnosis	Inflammation	Clinical Impression	Intensity at 337 nm	Red-Blue Ratio at 410 nm
1	Lateral tongue	CA	Mod	CA	Ab	Nml
		Nml	None	Nml	Nml	Nml
2	Ventral tongue	MRA	Mild	Ab-ND	Ab	Ab
		Nml	None	Nml	Nml	Nml
3	Lateral tongue	Dys	Min	CA	Nml	Ab
		Nml	None	Nml	Nml	Nml
4	Ventral tongue	CIS	NA	CA	Ab	Ab
		Nml	None	Nml	Nml	Nml
5	Ventral tongue	CA	Mod	CA	Ab	Ab
		CA	Mod	Ab-Dy	Ab	Nml
		Nml	Min	Nml	Nml	Nml
6	Buccal mucosa	Dys	Mod	CA	Ab	Ab
		Dys	Mod	Ab-ND	Ab	Nml
		Dys	None	Ab-ND	Ab	Ab
		Nml	None	Nml	Nml	Nml
7	Hard palate	Dys	NA	CA	Ab	Ab
		Nml	None	Nml	Nml	Nml
8	Ventral tongue	CIS	Sev	CA	Ab	Ab
		Dys	Mod	CA	Ab	Ab
		Nml	None	Nml	Nml	Nml
9	Gingiva	CA	Mild	CA	Ab	Ab
		Nml	Mild	Nml	Nml	Nml
	Buccal mucosa	CA	None	CA	Ab	Ab
		Nml	Yes	Nml	Nml	Nml
10	Lateral tongue	CA	Mild	CA	Ab	Ab
		CIS	Mod	CA	Ab	Ab
		Dys	Mild	Ab-ND	Nml	Ab
		Nml	Sev	Nml	Nml	Nml
11	Lateral tongue	CA	Mod	CA	NA	NA
		Dys	Mod	Nml	NA	NA
12	Floor of mouth	CA	Mod	CA	NA	NA
		CA	Mild	CA	NA	NA
		MRA	Mild	Nml	NA	NA
13	Ventral tongue	Dys	Mild	Nml	NA	NA
		MRA	Mod	CA	NA	NA
		MRA	Mild	CA	NA	NA
		MRA	Mild	CA	NA	NA
		Nml	Mod	Nml	NA	NA
14	Ventral tongue	Nml	None	Dys	NA	NA
		Dys	Yes	Dys	NA	NA
		Dys	Sev	Dys	NA	NA
		Nml	None	Nml	NA	NA
15	Retromolar trigone	CA	Mod	CA	NA	NA
		Dys	None	Nml	NA	NA
	Gingiva	Dys	Mod	Dys	NA	NA
		Nml	None	Nml	NA	NA

*CA indicates cancer; Nml, normal; MRA, mucosal reactive atypia; Dys, dysplasia; CIS, carcinoma in situ; Mod, moderate; Min, minimal; NA, not assessed; Sev, severe; Ab-ND, abnormal (not dysplastic); Ab-Dy, abnormal (dysplastic); and Ab, abnormal.

wavelengths: $P = .05$ for 337 nm (barely significant), $P = .23$ for 365 nm (not significant), and $P < .001$ for 410 nm (significant). However, most sites did not differ from each other. The Duncan multiple range test was used to determine which pairs of sites tend to differ. This method takes into account the number of tests made and controls the overall type I error rate to no more than 5%. These results are illustrated in Table 1. In general, the person-to-person variation at each site was greater than the contralateral variation within a particular site in the same person and the variation among different anatomical sites within the same person.

PATIENTS

Spectroscopic data were obtained from 45 sites in 15 patients. Data from 3 patients were excluded because of instrumentation error: the spectral readings were uninterpretable secondary to oversaturation of the diode array. In the remaining 12 patients, 33 sites were examined clinically, spectroscopically, and histologically (Table 2). In 2 patients, the clinically normal sites were abnormal on histological evaluation, preventing a comparison between normal and abnormal sites within these 2 patients.

Typical spectra from normal and abnormal areas are shown in **Figure 2**, A. The greatest intensity occurred

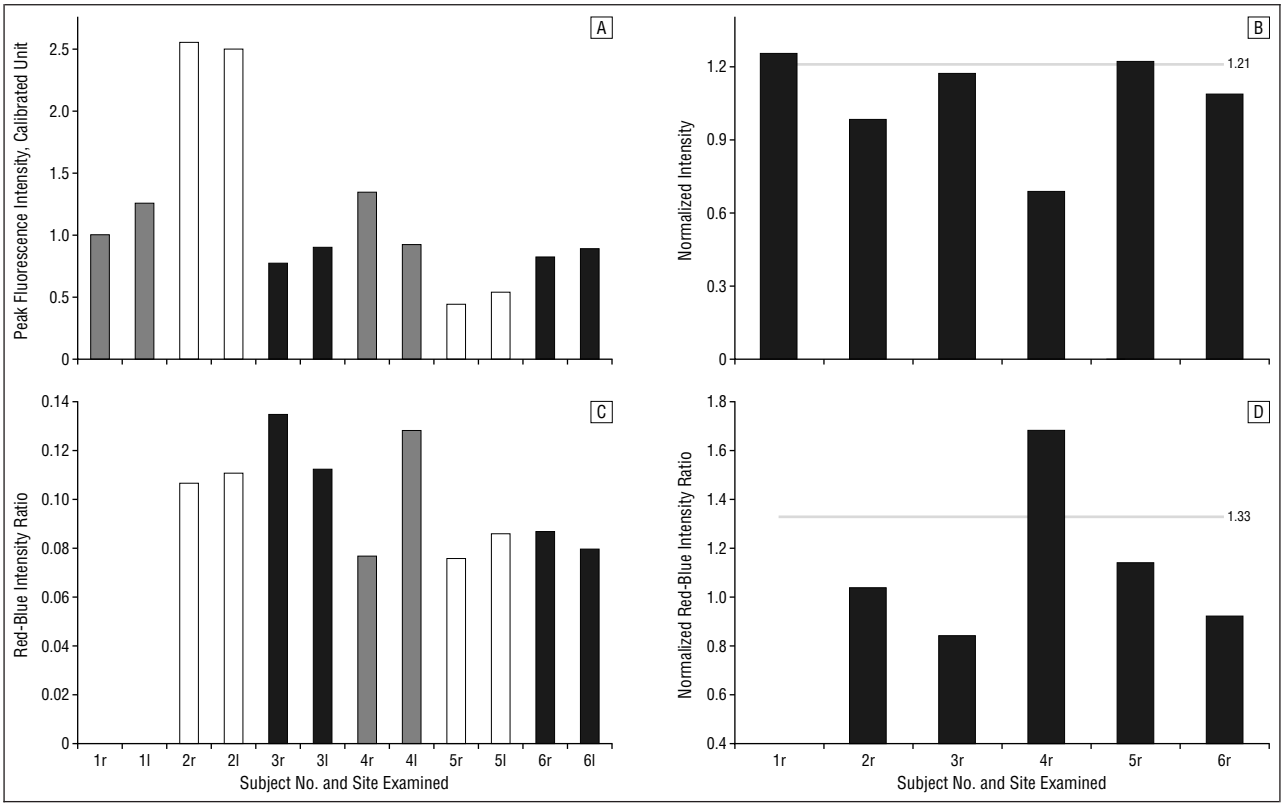

Figure 1. *A, Peak fluorescence intensities at the 337-nm excitation wavelength of bilateral tongue sites in 6 healthy volunteers. B, Peak intensities in (A) have been normalized to the right site value in each patient. The average normalized peak intensity of the left side was 1.06 within an SD of 0.121. A cutoff value of 1.21 (1 plus 1 SD) was chosen for normal for peak intensities at 337 nm. C, Peak fluorescence intensities in bilateral soft palate sites in 5 healthy volunteers at the 410-nm excitation wavelength. The data from patient 1 at this wavelength were unavailable because of investigator error. D, Data in (C) have been normalized to the right site value in each patient. A cutoff value of 1.22 (1 plus 1 SD) was chosen for normal for the 410-nm wavelength. r indicates right; l, left.*

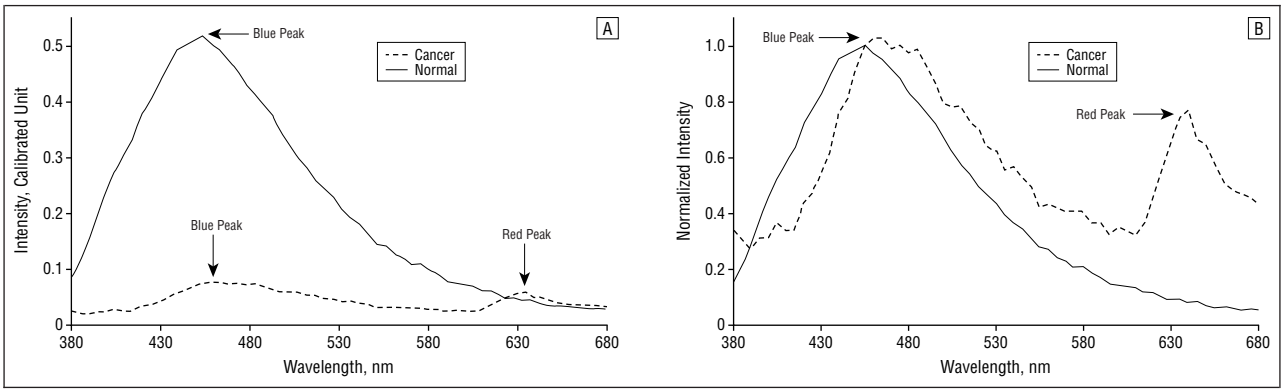

Figure 2. *A, Spectra obtained from normal and cancerous sites in 1 patient at the 365-nm excitation wavelength. B, Same data as in (A) except that the intensity of the cancer spectrum is now normalized to that of the spectrum from the normal sample. Note the shift of the peak intensity to a longer wavelength and the increased fluorescence of the abnormal tissue in the red region. Similar findings were obtained at 337- and 410-nm excitation wavelengths.*

in the blue region between 455 and 490 nm (blue peak). The blue peak from normal tissue is visibly greater than that from abnormal tissue. When the spectra of both areas were normalized (the line curves were adjusted so that the peak intensity of the abnormal and normal samples have the value of 1), changes in spectral line shape became evident (Figure 2, B). The line-shape differences were predominantly because of increased fluorescence of abnormal tissues in the red region (red peak at 635 nm) and a shift of the peak intensity of abnormal tissues to a longer wavelength. Spectra from all 3 wavelengths demonstrated consistent differences in peak intensity and spectral line shape between normal and abnormal tissue. The 365-nm excitation wavelength produced the least discrimination. Because the greatest spectral variance occurred in the blue (455-490 nm) and red (635 nm) regions, these 2 areas were chosen for further analysis.

To quantify the alterations in the spectra and to determine whether they were present in all patients, the intensities of the blue peaks of normal and abnormal sites were tabulated. For optimal data analysis, spectra should be obtained from contralateral normal and abnormal sites in each patient. This occurred in 10 of 12 evaluable pa-

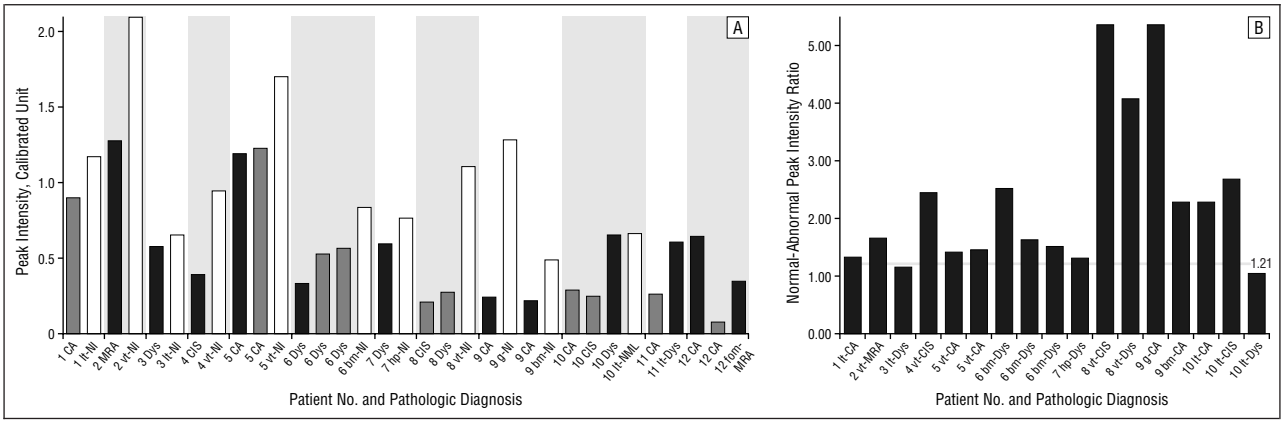

Figure 3. *A, Comparison of peak intensities of histologically abnormal samples (black bars) and histologically normal samples (white bars) at the 337-nm excitation wavelength. Although there is interpatient variability, the intensities of the abnormal samples are less than those of their normal control sample. B, A normal-abnormal peak intensity ratio is obtained by dividing each normal sample's peak intensity by the corresponding abnormal sample's peak intensity. In 15 of 17 sites, this ratio is greater than 1.21 (the calculated normal cutoff value from Figure 1, B). CA indicates cancer; lt, lateral tongue; NI, normal; MRA, mucosal reactive atypia; vt, ventral tongue; Dys, dysplasia; CIS, carcinoma in situ; bm, buccal mucosa; hp, hard palate; g, gingiva; and fom, floor of mouth.*

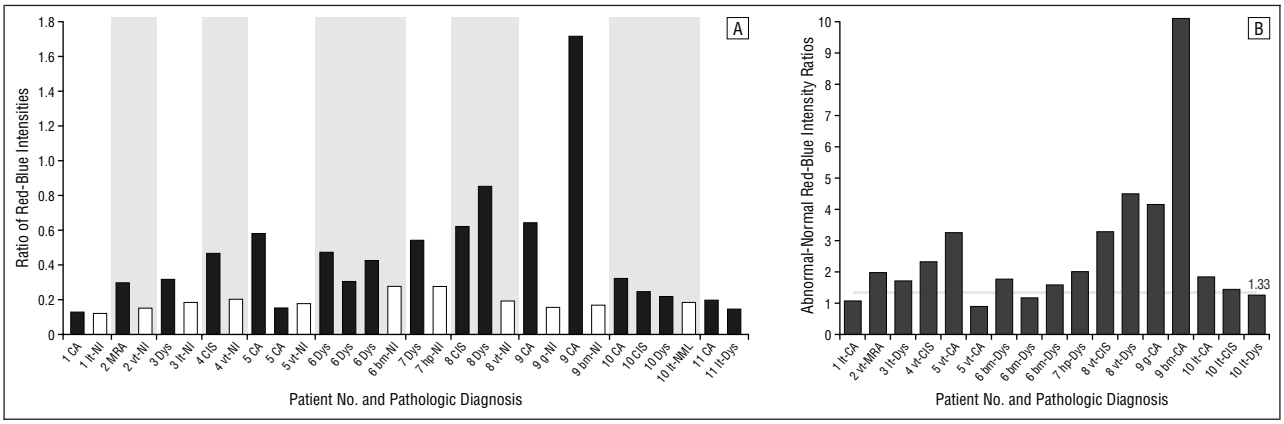

Figure 4. *A, Comparison of the ratio of intensities at the red (635-nm) and blue (490-nm) regions at the 410-nm excitation wavelength. Despite patient-to-patient variability, it is evident that this ratio in abnormal tissue (black bars) is greater than the ratio in the corresponding normal tissue (white bars). The data from patient 12 are missing for this wavelength because of investigator error. B, Ratio of abnormal red-blue intensity divided by normal red-blue intensity. This ratio was greater than 1.33 (the calculated normal cutoff value from Figure 1, D) in 13 of 17 sites. Abbreviations are explained in the legend to Figure 3.*

tients. The remaining 2 patients had clinically normal samples that were deemed dysplastic or mucosal reactive atypia on histological evaluation. The data from these 2 patients appear last in **Figure 3** and **Figure 4** and were not used in analyzing the sensitivity and specificity of the diagnostic algorithms.

Figure 3, A, shows the peak intensities of abnormal and normal samples at the 337-nm excitation wavelength. In 9 of 10 patient sites, the peak fluorescence intensities of normal sites were greater than those of all histologically abnormal sites; in the 10th patient, the peak intensity of the normal site was greater than that of 2 of 3 abnormal sites. Because of considerable patient-to-patient variation in intensity, the separation between normal and abnormal intensity peaks could be better visualized when the ratios of the peak intensities of normal areas to abnormal areas were calculated for each abnormal site (Figure 3, B). In 15 of 17 sites, this ratio was 1.21 or greater (1 plus 1 SD, as shown in Figure 1, B). The magnitude of the difference between normal and abnormal (the size of the ratio) did not seem to vary with increased severity of disease. Although results are shown only for the 337-nm excitation scans, similar results were obtained at all excitation wavelengths.

The ratios of the peak intensities in the red vs blue region (red-blue peak ratios) were also used to compare normal with abnormal tissues. The red-blue peak ratios were greater in abnormal tissues than in contralateral normal sites within the same patient (Figure 4, A). Again, patient-to-patient variation was high. As shown in Figure 4, B, the ratio of abnormal to normal red-blue peak ratios was greater than 1.00 in 16 of 17 sites. This ratio was greater than 1.33 (1 plus 1 SD) in 13 of 17 sites. Although results are shown only for the 410-nm excitation scans, similar results were obtained at all excitation wavelengths.

In **Figure 5**, the same data shown in Figures 3, B (x-axis), and 4, B (y-axis), are presented in a scattergram to illustrate the effect of combining these 2 algorithms based on the peak intensities at 337 nm and the red-blue peak ratios at 410 nm. Whereas each algorithm alone misclassified several abnormal sites as normal (ie, the abnormal site fell below the chosen normal cutoff value), when the 2 algorithms are combined, only 1 abnormal site was misclassified as normal by both algorithms.

Our data from healthy volunteers and patients suggest that fluorescence spectroscopy can be used to identify pathologic abnormalities in the oral mucosa. Using data from the first 10 patients in whom pathologic and spec-

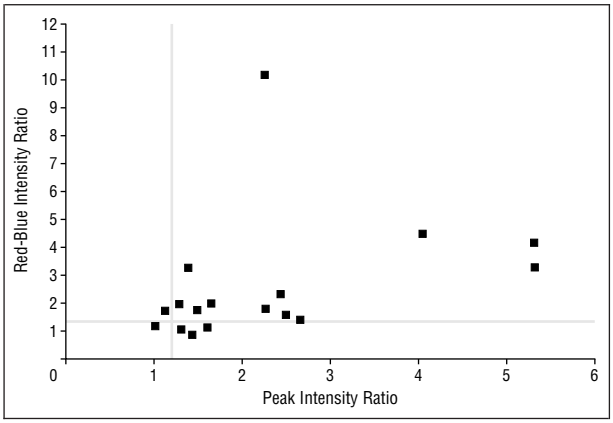

Figure 5. *Scattergram showing results from 2 spectroscopic algorithms. The normal-abnormal peak intensity ratio at 337 nm (Figure 3, B) is plotted on the x-axis and the normal-abnormal red-blue intensity ratio at 410 nm (Figure 4, B) is plotted on the y-axis. Note that 1 site falls completely below both normal cutoff values.*

troscopic data from an abnormal site and a corresponding normal site were available, we developed 2 simple diagnostic algorithms based on peak fluorescence intensity at the 337-nm excitation and the red-blue intensity ratio of the 410-nm excitation. A third diagnostic algorithm was made by combining the first 2 algorithms. A comparison of the sensitivity and specificity of these diagnostic algorithms is given in **Table 3**. The pathologic diagnosis was used as the criterion standard.

If the clinical diagnosis was normal or abnormal (not dysplastic) and the pathologic diagnosis was normal, then the clinical impression was characterized as a true-negative. Otherwise it was classified as a false-negative. If the clinical diagnosis was abnormal (dysplastic) or cancerous and the pathologic diagnosis was normal, then the clinical impression was classified as a false-positive. Otherwise it was classified as a true-positive. Using these criteria, visual examination by an experienced practitioner (A.G. and R.J.) detected oral neoplasia or dysplasia with a sensitivity and specificity of 76.5% and 100.0%, respectively. All study patients had been referred to a cancer center because of a pathologic diagnosis or suspicion of cancer, and this most likely affected the clinician's index of suspicion for malignant lesions.

Figure 1, B, shows that the normalized peak intensity of 4 of 6 normal sites at the 337-nm excitation is less than 1 plus 1 SD (1.21). Using this value as a cutoff point to classify unknown sites as normal or abnormal yielded a sensitivity of 88.2% and a specificity of 100.0%. Similarly, Figure 1, D, shows that the normalized red-blue peak ratio at 410 nm of all but 1 site is less than 1 plus 1 SD (1.33). Using this value as a cutoff point to classify unknown sites as normal or abnormal gave a sensitivity of 76.5% and a specificity of 100.0%. Combining these 2 criteria, and identifying those samples as abnormal that exceed at least 1 criterion, yielded a sensitivity of 94.1%, an increase compared with the sensitivity of each algorithm alone.

Table 3. Sensitivity and Specificity of 3 Spectroscopic Diagnostic Algorithms

	Sensitivity, %	Specificity, %
Clinical impression	76.5	100.0
Normalized peak intensity at 337 nm	88.2	100.0
Normalized red-blue peak ratio at 410 nm	76.5	100.0
Combined normalized peak intensity at 337 nm and red-blue peak ratio at 410 nm	94.1	100.0

	Pathologic Diagnosis	
	Abnormal	Normal
Clinical impression		
Abnormal	13	0
Normal	4	11
Spect 337		
Abnormal	15	0
Normal	2	11
Spect 410		
Abnormal	13	0
Normal	4	11
Spect 337 + 410		
Abnormal	16	0
Normal	1	11

COMMENT

The results of this study demonstrate the ability of fluorescence spectroscopy to differentiate between neoplastic and nonneoplastic oral cavity tissue in vivo. Comparisons of neoplastic and nonneoplastic sites within patients revealed differences in spectral intensities and line shapes at 3 excitation wavelengths (337, 365, and 410 nm) that may be exploited to noninvasively identify neoplastic oral lesions. In general, the peak fluorescence intensities of abnormal sites were less than those of normal sites. The fluorescence intensities of abnormal sites were increased in the red spectral region compared with those of normal sites. Although differences were noted at all 3 wavelengths, the 337- and 410-nm wavelengths provided the best discrimination between normal and abnormal in this study.

The specific alterations in tissue architecture or biochemical composition causing the overall decrease in fluorescence intensity of neoplastic and dysplastic tissue have not been elucidated. Natural fluorophores that may undergo changes in quantity or form during neoplastic progression include flavins, nicotinamide adenine dinucleotide (NADH), and collagen.[9] Some decreased fluorescence intensity of abnormal specimens, as illustrated in Figure 2, may be attributed to an increase in hemoglobin absorption.

Our results confirm and expand the findings of previous investigations. Dhingra et al[10] analyzed spectra from oral cavity lesions obtained in vivo at the 370- and 410-nm excitation wavelengths. As in the present study, this group also found decreased peak intensities in pathologically abnormal vs normal tissues and increased intensity in the red region of abnormal vs normal tissues. An assessment of the sensitivity and specificity of diagnostic algorithms using these wavelengths was not presented, however. An earlier clinical trial by Savage et al[11] measured 2 fluorescence emission spectra at the 300- and 340-nm excitation and 2 excitation spectra at 380- and 450-nm

emission from healthy volunteers and patients with lateral tongue cancer. This group used intensity ratios at various wavelengths (including the red-blue ratio) to discriminate between malignant and normal tongue tissue; no dysplastic lesions were examined.

In addition, results of an in vitro study of oral mucosa by Roy et al[12] also showed consistent spectral differences when dysplastic and cancerous tissue were compared with normal tissue. This group found that spectral differences were most prominent at the 410-nm excitation wavelength. All abnormal spectra exhibited increased fluorescence in the red region (>600 nm). Similar results were presented by Ingrams et al.[13]

In our investigation, the 410-nm excitation wavelength produced the greatest number of red shifts (peaks of abnormal samples in the 635-nm region), which, when used in conjunction with the lower peak intensities in the blue region of the neoplastic tissue, provide an excellent signature for abnormal samples. Because only 3 wavelengths were evaluated, the possibility remains that other wavelengths not yet tested would provide greater discrimination between normal, inflammatory, and neoplastic tissue. Unlike in other studies (Roy et al[12]), a visible red shift did not occur for all our subjects, but it was noted more frequently at the 410-nm excitation wavelength. The exact cause of the red shift is not known, although currently it is attributed to porphyrins.[14,15] The fluorescence maximum of porphyrin is closest to the 410-nm excited spectra obtained in this study. It remains unclear whether the red shift is caused by increased porphyrin content within cancerous cells or some other cause, such as increased porphyrin secondary to bacterial synthesis within necrotic tissue. Several bacteria, such as *Escherichia coli, Klebsiella pneumonia,* and *Staphylococcus pyogenes,* among others, are known to produce porphyrin and to induce red fluorescence.[14]

The results of this study are important because they demonstrate the diagnostic potential of fluorescence spectroscopy for the diagnosis of early neoplastic lesions of the oral mucosa. The development of an optical spectroscopy system that can differentiate normal, inflammatory, and neoplastic samples based on autofluoresence alone would be a tremendous clinical advance. By avoiding the need for introduction of exogenous dyes, invasive procedures, and clinical diagnostic experience, this technology could make possible low-cost mass screening for oral neoplasia in settings such as primary care and dental clinics. In addition, in patients with previous malignant lesions of the aerodigestive tract, such a system could greatly augment the ability to adequately follow up patients for the development of second primary lesions.

However, the data presented in this report were obtained from a small number of volunteers and patients. The algorithms developed so far seem promising for discriminating between normal and abnormal tissue, but they cannot distinguish between mucosal reactive atypia, dysplasia, and frank carcinoma. In addition, the algorithms require a comparison of abnormal tissue to a corresponding normal site within the same patient. Any method developed for analysis should take into account that the patient-to-patient variation of healthy volunteers is great and that the variation within a particular location in each person is small. Thus, any comparison of normal to abnormal tissues should focus within a single patient. The need exists for further study with more patients and volunteers to develop diagnostic algorithms that can adequately differentiate between normal, inflammatory, premalignant, and malignant oral mucosal tissue.

Accepted for publication September 15, 1997.

Presented at the 4th International Conference on Head and Neck Cancer, Toronto, Ontario, August 1, 1996.

We thank Glenn Criswell and the patients and staff of the Department of Head and Neck Surgery, The University of Texas M. D. Anderson Cancer Center, Houston, for assistance with data acquisition and Jude Richard for editorial assistance.

Reprints: Ann Gillenwater, MD, Department of Head and Neck Surgery, The University of Texas M. D. Anderson Cancer Center, 1515 Holcombe Blvd, Box 69, Houston, TX 77030.

REFERENCES

1. Silverman S, Migliorati C, Barbosa J. Toluidine blue staining in the detection of oral precancerous and malignant lesions. *Oral Surg Oral Med Oral Pathol.* 1984; 57:379-382.
2. Rosenberg D, Cretin S. Use of meta-analysis to evaluate tolonium chloride in oral cancer screening. *Oral Surg Oral Med Oral Pathol.* 1987;67:621-627.
3. Epstein J, Scully C, Spinelli J. Toluidine blue and Lugol's iodine application in the assessment of oral malignant disease and lesions at risk of malignancy. *J Oral Pathol Med.* 1992;21:160-163.
4. Romer TJ, Fitzmaurice M, Cothren RM, et al. Laser-induced fluorescence microscopy of normal colon and dysplasia in colonic adenomas: implications for spectroscopic diagnosis. *Am J Gastroenterol.* 1995;90:81-87.
5. Ramanujam N, Mitchell MF, Mahadevan A, et al. In vivo diagnosis of cervical intraepithelial neoplasia using 337 nm excited laser-induced fluorescence. *Proc Natl Acad Sci U S A.* 1994;91:10193-10197.
6. Ramanujam N, Mitchell MF, Mahadevan A, et al. Development of a multivariate statistical algorithm to analyze human cervical tissue fluorescence spectra acquired in vivo. *Lasers Surg Med.* 1996;19:46-62.
7. Hung J, Lam S, LeRiche JC, Palcic B. Autofluorescence of normal and malignant bronchial tissue. *Lasers Surg Med.* 1991;11:99-105.
8. Alfano RR, Pradhan A, Tang GC. Optical spectroscopic diagnosis of cancer and normal breast tissues. *J Opt Soc Am A.* 1989;6:1015-1023.
9. Richards-Kortum R, Sevick-Muraca E. Quantitative optical spectroscopy for tissue diagnosis. *Annu Rev Phys Chem.* 1996;47:555-606.
10. Dhingra JK, Perrault DF Jr, McMillan K,et al. Early diagnosis of upper aerodigestive tract cancer by autofluorescence. *Arch Otolaryngol Head Neck Surg.* 1996; 122:1181-1186.
11. Savage H, Kolli V, Ansley J, Chandawarkar R, Alfano R, Schantz S. Innate tissue fluorescence of the oral mucosa of controls and head and neck cancer patients. In: Alfano RR, ed. *Proceedings of Advances in Laser and Light Spectroscopy to Diagnose Cancer and Other Diseases II.* Bellingham, Wash: SPIE; 1995;2387:2-14.
12. Roy K, Bottril I, Ingrams D, et al. Diagnostic fluorescence spectroscopy of oral mucosa. In: Anderson R, ed. *Proceedings in Lasers in Surgery: Advance Characterization, Therapeutics and Systems V.* Bellingham, Wash: SPIE; 1995;2395: 135-142.
13. Ingrams DR, Dhingra JK, Roy K, et al. Autofluorescence characteristics of oral mucosa. *Head Neck.* 1997;19:27-32.
14. Harris D, Werkhaven J. Endogenous porphyrin fluorescence in tumors. *Lasers Surg Med.* 1987;7:467-472.
15. Konig K, Schneckenburger H, Hemmer J, Tromberg B, Steiner R. In vivo fluorescence detection and imaging of porphyrin-producing bacteria in the human skin and oral cavity for the diagnosis of acne vulgaris, caries, and squamous cell carcinoma. In: Alfano RR, ed. *Proceedings of Advances in Laser and Light Spectroscopy to Diagnose Cancer and Other Diseases.* Bellingham, Wash: SPIE; 1994; 2135:129-138.